Alexandria Engineering Journal (2015) 54, 733–743

HOSTED BY

Alexandria University

Alexandria Engineering Journal

www.elsevier.com/locate/aej
www.sciencedirect.com

ORIGINAL ARTICLE

Effect of heat sink/source on peristaltic flow of Jeffrey fluid through a symmetric channel

M. Rehman [a], S. Noreen [b,*], A. Haider [c], H. Azam [d]

[a] Department of Mathematics, University of Management and Technology, Lahore 54770, Pakistan
[b] Comsats Institute of Information Technology, Park Road, 44000 Islamabad, Pakistan
[c] Department of Electrical Engineering, University of Management and Technology, Lahore 54770, Pakistan
[d] Department of Mathematics, Syed babar Ali School of Science and Engineering, LUMS, Lahore, Pakistan

Received 18 July 2014; revised 11 February 2015; accepted 10 March 2015
Available online 24 April 2015

KEYWORDS

Peristaltic flow;
Heat transfer;
Jeffrey parameter λ_1;
Heat sink/source parameter β_1;
Material parameter α

Abstract The peristaltic flow and heat transfer through a symmetric channel in the presence of heat sink/source parameter have been analyzed in this paper. It also deals with the effect of the natural convection coefficient in the momentum equation. Low Reynolds number and small wave number approximation are used to convert the non-linear partial differential equations into the non-linear ordinary differential equations. In order to solve the governing model, perturbation method has been chosen by taking α (material parameter) as a small parameter. Expressions have been obtained for temperature, velocity, stream function, pressure rise and frictional forces. The features of the flow characteristics are analyzed by plotting graphs and the results are discussed in details. It has been observed that velocity increases with an increase of α (material parameter). The peristaltic pumping and in the copumping region the pumping rate decreases by increasing the value of α (material parameter). The size of the trapped bolus decreases by increasing the value of α (material parameter). The temperature profile increases by increasing the value of β_1 (heat sink/source parameter).

1. Introduction

Heat transfer occurs in almost all branches of Engineering and Biosciences. Also, it has many industrial, chemical, residential and commercial applications. It is well-known heat transfer follows the first law of thermodynamics.

Peristaltic transport is a means of fluid flow in elastic path by the way of contraction and expansion processes. This flow induces progressive waves along the elastic path. Peristaltic transport is an inbuilt mechanism in many biological systems including human body such as: transportation of biofluids, spermatozoa in the ducts efferent of the male reproductive tract, ovum in the female fallopian tube, lymph in the lymphatic vessel and also in many other glandular ducts. Technical roller and finger pumps also operate according to the peristaltic principle. Further it is also used in transporting sensitive or corrosive fluids, sanitary fluids and noxious fluids in nuclear industry. The first systematic investigation of

* Corresponding author.
E-mail address: laurel_lichen@yahoo.com (S. Noreen).
Peer review under responsibility of Faculty of Engineering, Alexandria University.

http://dx.doi.org/10.1016/j.aej.2015.03.011

peristaltic measure has been carried out by Latham [1]. Later on more researches carried out this work [2–5].

For the occurrence of heat transfer with peristaltic flow, there must be transport of fluid by contraction and expansion involving kinetic energy. The peristaltic propulsion will result into the transfer of heat. Some other examples include: drying, evaporation, cooling, combustion of fuel droplets and ablation cooling, vehicles sourcing, reentry and even ordinary vents such as rain, snow melts and hail. Keeping in view of its importance and real world validity several researchers [6–10] have studied the effects of heat transfer on peristaltic transport of Newtonian and non-Newtonian fluids.

Some recent researches are as follows: Vasudev et al. has investigated the effects of heat transfer on the peristaltic flow of Jeffrey fluid through a porous medium in a vertical annulus [11]. Khan et al. have presented the peristaltic transport of a Jeffrey fluid with variable viscosity through a porous medium in an asymmetric channel [12]. Akram et al. have discussed the significance of Nanofluid and partial slip on the peristaltic transport of a Non-Newtonian fluid with different waveforms [13]. Pandey has presented the unsteady model of transportation of Jeffrey fluid by peristalsis [14]. Akbar et al. have analyzed the thermal and velocity slip effects on the MHD peristaltic flow with carbon nanotubes in an asymmetric channel: application of radiation therapy [15]. Noreen has studied the numerical solution of the effects of induced magnetic field on Jeffrey six-constant fluid with peristaltic flow [16].

Also several works available in the literature deal with passage arrangement optimization in plate-fin heat exchangers such as [25–27].

This paper considers Jeffrey six-constant fluid with heat transfer. The Jeffrey model is relatively simple linear model using time derivatives instead of convected derivatives e.g., the Oldroyd-B model, and it represents a rheology different from Newtonian fluid. The whole analysis has been carried out in a moving frame of reference. The governing equations of fluid flow are solved subject to relevant boundary conditions. Perturbation solutions of pressure gradient, stream function and temperature distribution are obtained. Graphs are plotted for different parameters.

2. Indispensable equations

The constitutive equations for Jeffrey six-constant fluid model are [17]

$$\nabla \cdot \mathbf{V} = 0, \tag{1}$$

$$\rho \frac{d\mathbf{V}}{dt} = \nabla \cdot \mathbf{T}' + \rho \mathbf{b_f} + \mathbf{R}, \tag{2}$$

$$\rho C_p \frac{dT}{dt} = k\nabla^2 T + Q_0, \tag{3}$$

and the Cauchy stress Tensor is

$$\mathbf{T}' = -p\mathbf{I} + \mathbf{S}, \tag{4}$$

$$\mathbf{S} + \lambda_1 \left[\frac{d\mathbf{S}}{dt} - W\mathbf{S} + \mathbf{S}W + \breve{a}(\mathbf{S}D + D\mathbf{S}) + \breve{b}\mathbf{S} : DI + \breve{c}Dtr\mathbf{S} \right] = 2\mu \left[D + \lambda_2 \left(\frac{dD}{dt} - WD + DW + 2\breve{a}DD + \breve{b}D : DI \right) \right], \tag{5}$$

$$\mathbf{L} = \text{grad } \mathbf{V}, \tag{6}$$

$$\mathbf{A}_1 = \mathbf{L} + \mathbf{L}^T. \tag{7}$$

Here, $\mathbf{V}$ is the velocity vector, $\mathbf{b_f}$ is the body force (assumed to be zero), $\mathbf{R}$ is the Darcy's resistance (assumed to be zero), ρ is the fluid density, $\mathbf{S}$ is the extra stress tensor, $\mathbf{T}'$ is the Cauchy stress tensor, C_p is the specific heat, T is the temperature, k is the constant thermal conductivity, $Q_0 > 0$ is the heat source and $Q_0 < 0$ is the heat sink, p is the pressure, $D = \frac{(\nabla \mathbf{V}' + \nabla \mathbf{V})}{2}$ is the symmetric part of $\nabla \mathbf{V}$, $W = \frac{(\nabla \mathbf{V}' - \nabla \mathbf{V})}{2}$ is the antisymmetric part of $\nabla \mathbf{V}$, λ_1 and λ_2 are the relaxation and delay times respectively, μ is the dynamic viscosity, $\frac{d}{dt}$ is the material derivative, and $\breve{a}, \breve{b}$ and $\breve{c}$ are arbitrary material constants.

3. Formulation of the problem

Consider the steady and incompressible flow of Jeffrey fluid in symmetric channel. The surface is maintained at uniform constant temperature (Fig. 1).

The motion of an incompressible fluid is caused by sinusoidal wave trains propagating with constant speed c along the channel wall as given by the following:

$$h'(X', t') = a + b \sin\left(\frac{2\pi}{\lambda}(X' - ct')\right). \tag{8}$$

In above equation, b is the amplitude of the waves and $2a$ is the channel width, λ is the wavelength. X' and Y' are the rectangular Cartesian coordinates. The wall $Y = h'$ is kept at a temperature T_0. Introducing a wave frame (x', y') moves with velocity c away from the fixed frame (X', Y') with velocity c by the transformation

$$x' = X' - ct, \quad y' = Y', \quad u'(x', y') = U'(X', Y', t') - c, \quad v'(x', y') = V'(X', Y', t'), \tag{9}$$

where (u', v') are the velocity components in the wave frame (x', y'). The equations governing the fluid motion in the wave frame are as follows:

$$\frac{\partial u'}{\partial x'} + \frac{\partial v'}{\partial y'} = 0, \tag{10}$$

$$\rho \left[u' \frac{\partial}{\partial x'} + v' \frac{\partial}{\partial y'} \right] u' = -\frac{\partial p'}{\partial x'} + \frac{\partial S'_{xx'}}{\partial x'} + \frac{\partial S'_{xy'}}{\partial y'} + \rho g \beta_T (T - T_0), \tag{11}$$

$$\rho \left[u' \frac{\partial}{\partial x'} + v' \frac{\partial}{\partial y'} \right] v' = -\frac{\partial p'}{\partial y'} + \frac{\partial S'_{yx'}}{\partial x'} + \frac{\partial S'_{yy'}}{\partial y'}, \tag{12}$$

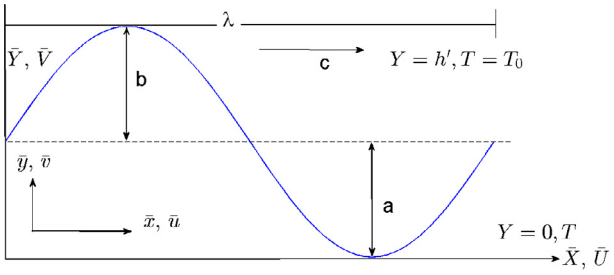

Figure 1 Flow geometry.

$$\rho C_p\left[u'\frac{\partial}{\partial x'}+v'\frac{\partial}{\partial y'}\right]T'=k\left[\frac{\partial^2 T'}{\partial x'^2}+\frac{\partial^2 T'}{\partial y'^2}\right]+Q_0. \tag{13}$$

Next, we introduce the following dimensionless quantities:

$$x=\frac{x'}{\lambda},\quad y=\frac{y'}{a},\quad u=\frac{u'}{c},\quad v=\frac{v'}{c},$$
$$S_{ij}=\frac{aS'_{ij}}{\mu c}\ (\text{for } i,j=1,2,3),\quad Re=\frac{\rho ca}{\mu},\quad \lambda=\frac{\Lambda_1 c}{a},\quad \delta=\frac{a}{\lambda},$$
$$p=\frac{a^2p'}{\lambda\mu c},\quad h=\frac{h'}{a},\quad u=\frac{\partial\psi}{\partial y},\quad v=-\delta\frac{\partial\psi}{\partial x},\quad Pr=\frac{\mu C_p}{k}$$
$$\gamma=\frac{T'-T_0}{T_0},\quad \beta_1=\frac{Q_0a^2}{kT_0},\quad Gt=\frac{\beta_T gT_0}{cv}, \tag{14}$$

where Pr, δ, Re, and Gr are the Prandtl, wave, Reynolds numbers and Local Grashof number respectively; β_1 is the heat sink/source parameter. Using dimensionless variables as in (14) and introducing stream function ψ, Eqs. (10)–(13) become as follows:

$$u=\frac{\partial\psi}{\partial y},\quad v=-\delta\frac{\partial\psi}{\partial x}, \tag{15}$$

$$Re\delta\left[\left(\frac{\partial\psi}{\partial y}\frac{\partial}{\partial x}-\frac{\partial\psi}{\partial x}\frac{\partial}{\partial y}\right)\frac{\partial\psi}{\partial y}\right]=-\frac{\partial p}{\partial x}+\delta\frac{\partial S_{xx}}{\partial x}+\frac{\partial S_{xy}}{\partial y}+Gt\gamma, \tag{16}$$

$$-\delta^3 Re\left[\left(\frac{\partial\psi}{\partial y}\frac{\partial}{\partial x}-\frac{\partial\psi}{\partial x}\frac{\partial}{\partial y}\right)\frac{\partial\psi}{\partial x}\right]=-\frac{\partial p}{\partial y}+\delta\frac{\partial S_{yy}}{\partial y}+\delta^2\frac{\partial S_{yx}}{\partial x}, \tag{17}$$

$$\delta PrRe\left[\frac{\partial\psi}{\partial y}\frac{\partial\gamma}{\partial x}-\frac{\partial\psi}{\partial x}\frac{\partial\gamma}{\partial y}\right]=\delta^2\frac{\partial^2\gamma}{\partial x^2}+\frac{\partial^2\gamma}{\partial y^2}+\beta_1. \tag{18}$$

The values of S_{xx}, S_{xy}, S_{yy} and S_{yx} can be obtained from Noreen [16]. By eliminating p from the Eqs. (16) and (17), the following equation can be obtained:

$$\delta Re\left[\left(\frac{\partial\psi}{\partial y}\frac{\partial}{\partial x}-\frac{\partial\psi}{\partial x}\frac{\partial}{\partial y}\right)\left(\frac{\partial^2\psi}{\partial y^2}+\delta^2\frac{\partial^2\psi}{\partial x^2}\right)\right]$$
$$=\delta\frac{\partial^2}{\partial x\partial y}(S_{xx}-S_{yy})+\left(\frac{\partial^2}{\partial y^2}-\delta^2\frac{\partial^2}{\partial x^2}\right)S_{xy}+Gt\frac{\partial\gamma}{\partial y}. \tag{19}$$

The boundary conditions are as follows:

$$\psi=0,\quad y=0,$$
$$\psi=F,\quad y=h(x)=1+a\sin[2\pi x],$$
$$\frac{\partial^2\psi}{\partial y^2}=0\quad \text{at } y=0\quad \text{and}\quad \frac{\partial\psi}{\partial y}=-1\quad \text{at } y=h,$$
$$\frac{\partial\gamma}{\partial y}=0,\quad \text{at } y=0,\quad \gamma=1,\quad \text{at } y=h. \tag{20}$$

4. Rate of volume flow rate and boundary conditions

In fixed frame, the dimensional volume flow is defined by

$$Q'=\int_0^{h'(X',t')}U'(X',Y',t')dY'. \tag{21}$$

The rate of volume flow in the wave frame is given by

$$q=\int_0^{h'}u(x',y')dy'. \tag{22}$$

Substituting Eq. (9) into Eq. (21) and making use of Eq. (22), we find that the two rates of volume flow rate are related through

$$Q=q+ch'(x'). \tag{23}$$

The time-mean flow over a period T is defined as

$$\bar{Q}=\frac{1}{T}\int_0^T Qdt. \tag{24}$$

Substituting Eq. (23) into Eq (24), and integrating, we get

$$Q'=q'+ac. \tag{25}$$

The dimensionless time-mean flow θ in the fixed and F in the wave frame are defined as

$$\theta=\frac{Q'}{ac}\quad \text{and}\quad F=\frac{q}{ac}. \tag{26}$$

Rewriting Eq. (25)

$$\theta=F+1, \tag{27}$$

where

$$F=\int_0^{h(x)}\frac{\partial\psi}{\partial y}dy=\psi(h(x))-\psi(0), \tag{28}$$

The dimensionless form of $h'(X',t')$ is

$$h(x)=1+a\sin[2\pi x]. \tag{29}$$

For long wavelength and low Reynolds number approximation i.e., ($\delta\ll 1, Re\ll 1$), the Eqs. (16)–(19) can be written as follows:

$$\frac{\partial p}{\partial x}=\frac{\partial S_{xy}}{\partial y}+Gt\gamma, \tag{30}$$
$$\frac{\partial p}{\partial y}=0, \tag{31}$$
$$\frac{\partial^2 S_{xy}}{\partial y^2}+Gt\frac{\partial\gamma}{\partial y}=0, \tag{32}$$
$$\frac{\partial^2\gamma}{\partial y^2}+\beta_1=0, \tag{33}$$

where

$$S_{xy}=\frac{\partial^2\psi}{\partial y^2}\left(\frac{1-\frac{\lambda_1\lambda_2}{2}\alpha\left(\frac{\partial^2\psi}{\partial y^2}\right)^2}{1-\frac{\lambda_1^2}{2}\alpha\left(\frac{\partial^2\psi}{\partial y^2}\right)^2}\right), \tag{34}$$
$$\alpha=\breve{b}\breve{c}+(-1+\breve{a}+\breve{c})(1+\breve{a}+\breve{b}). \tag{35}$$

Making use of Eqs. (34) and (35), Eqs. (30) and (32) become

$$\frac{\partial p}{\partial x}=\frac{\partial}{\partial y}\left[\frac{\partial^2\psi}{\partial y^2}\left(\frac{1-\frac{\lambda_1\lambda_2}{2}\alpha\left(\frac{\partial^2\psi}{\partial y^2}\right)^2}{1-\frac{\lambda_1^2}{2}\alpha\left(\frac{\partial^2\psi}{\partial y^2}\right)^2}\right)\right]+Gt\gamma, \tag{36}$$

$$\frac{\partial^2}{\partial y^2}\left[\frac{\partial^2\psi}{\partial y^2}\left(\frac{1-\frac{\lambda_1\lambda_2}{2}\alpha\left(\frac{\partial^2\psi}{\partial y^2}\right)^2}{1-\frac{\lambda_1^2}{2}\alpha\left(\frac{\partial^2\psi}{\partial y^2}\right)^2}\right)\right]+Gt\frac{\partial\gamma}{\partial y}=0, \tag{37}$$

Further, applying binomial expansion about α, Eqs. (36) and (37) can be as follows:

$$\frac{\partial^4\psi}{\partial y^4}+\alpha A\frac{\partial^2}{\partial y^2}\left(\frac{\partial^2\psi}{\partial y^2}\right)^3+\alpha^2 B\frac{\partial^2}{\partial y^2}\left(\frac{\partial^2\psi}{\partial y^2}\right)^5+Gt\frac{\partial\gamma}{\partial y}=0, \tag{38}$$

$$\frac{\partial p}{\partial x}=\frac{\partial}{\partial y}\left[\frac{\partial^2\psi}{\partial y^2}+\alpha A\left(\frac{\partial^2\psi}{\partial y^2}\right)^3+\alpha^2 B\left(\frac{\partial^2\psi}{\partial y^2}\right)^5\right]+Gt\gamma, \tag{39}$$

$$\frac{\partial^2\gamma}{\partial y^2}+\beta_1=0, \tag{40}$$

where A and B are the material parameters for Jeffrey fluid defined by

$$A=\frac{3}{2}\lambda_1^2-\frac{1}{2}\lambda_1\lambda_2,\quad B=-\frac{3}{4}\lambda_1^3\lambda_2. \tag{41}$$

5. Perturbation solution

To obtain the closed form solution of the Eqs. (38)–(40) for any arbitrary set of values of various parameters, the power series expansion about the material parameter α has been employed to obtain the following:

$$\psi=\psi_0+\alpha\psi_1+\alpha^2\psi_2+O(\alpha^3),$$
$$\frac{dp}{dx}=\frac{dp_0}{dx}+\alpha\frac{dp_1}{dx}+\alpha^2\frac{dp_2}{dx}+O(\alpha^3),$$
$$S_{xx}=S_{0xx}+\alpha S_{1xx}+\alpha^2 S_{2xx}+O(\alpha^3),$$
$$S_{yy}=S_{0yy}+\alpha S_{1yy}+\alpha^2 S_{2yy}+O(\alpha^3),$$
$$S_{xy}=S_{0xy}+\alpha S_{1xy}+\alpha^2 S_{2xy}+O(\alpha^3),$$
$$F=F_0+\alpha F_1+\alpha^2 F_2+O(\alpha^3),$$
$$p=p_0+\alpha p_1+\alpha^2 p_2+O(\alpha^3),$$
$$\gamma=\gamma_0+\alpha\gamma_1+\alpha^2\gamma+O(\alpha^3). \tag{42}$$

Inserting Eq. (42) into Eqs. (38)–(40) we get the following systems:

5.1. Zero order system

$$\frac{\partial^4\psi_0}{\partial y^4}+Gt\frac{\partial\gamma_0}{\partial y}=0, \tag{43}$$

$$\frac{\partial p_0}{\partial x}=\frac{\partial}{\partial y}\left[\frac{\partial^2\psi_0}{\partial y^2}\right]+Gt\gamma_0, \tag{44}$$

$$\frac{\partial^2\gamma_0}{\partial y^2}+\beta_1=0, \tag{45}$$

$$\psi_0=0,\quad \frac{\partial^2\psi_0}{\partial y^2}=0,\quad \frac{\partial\gamma_0}{\partial y}=0,\quad \text{at } y=0, \tag{46}$$

$$\psi_0=F_0,\quad \frac{\partial\psi_0}{\partial y}=-1,\quad \gamma_0=0,\quad \text{at } y=h(x). \tag{47}$$

5.2. First order system

$$\frac{\partial^4\psi_1}{\partial y^4}+A\frac{\partial^2}{\partial y^2}\left(\frac{\partial^2\psi_0}{\partial y^2}\right)^3+Gt\frac{\partial\gamma_1}{\partial y}=0, \tag{48}$$

$$\frac{\partial p_1}{\partial x}=\frac{\partial}{\partial y}\left[\frac{\partial^2\psi_1}{\partial y^2}+A\left(\frac{\partial^2\psi_0}{\partial y^2}\right)^3\right]+Gt\gamma_1, \tag{49}$$

$$\frac{\partial^2\gamma_1}{\partial y^2}=0,$$

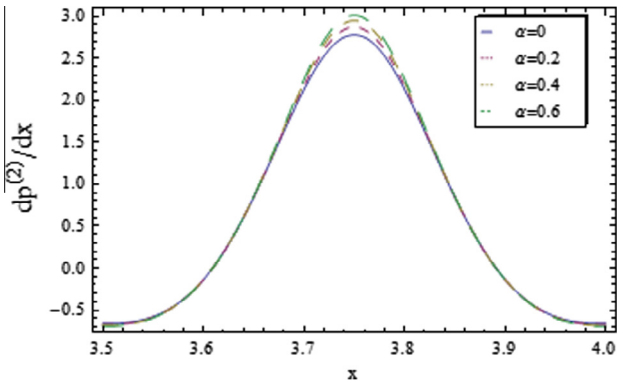

Figure 2 Influence of α on $dp^{(2)}/dx$ when $a=0.45, \beta_1=0.9, Gt=0.67, \theta=0.3, \lambda_1=0.4, \lambda_2=0.5$.

$$\psi_1=0,\quad \frac{\partial^2\psi_1}{\partial y^2}=0,\quad \frac{\partial\gamma_1}{\partial y}=0,\quad \text{at } y=0, \tag{50}$$

$$\psi_1=F_1,\quad \frac{\partial\psi_1}{\partial y}=0,\quad \gamma_1=0,\quad \text{at } y=h(x). \tag{51}$$

5.3. Second order system

$$\frac{\partial^4\psi_2}{\partial y^4}+3A\frac{\partial^2}{\partial y^2}\left[\left(\frac{\partial^2\psi_0}{\partial y^2}\right)^2\left(\frac{\partial^2\psi_1}{\partial y^2}\right)\right]+B\frac{\partial^2}{\partial y^2}\left(\frac{\partial^2\psi_0}{\partial y^2}\right)^5+Gt\frac{\partial\gamma_2}{\partial y}=0,$$

$$\frac{\partial p_2}{\partial x}=\frac{\partial}{\partial y}\left[\frac{\partial^2\psi_2}{\partial y^2}+3A\left(\frac{\partial^2\psi_0}{\partial y^2}\right)^2\left(\frac{\partial^2\psi_1}{\partial y^2}\right)+B\left(\frac{\partial^2\psi_0}{\partial y^2}\right)^5\right]+Gt\gamma_2,$$

$$\frac{\partial^2\gamma_2}{\partial y^2}=0,$$

$$\psi_2=0,\quad \frac{\partial^2\psi_2}{\partial y^2}=0,\quad \frac{\partial\gamma_2}{\partial y}=0,\quad \text{at } y=0, \tag{52}$$

$$\psi_2=F_2,\quad \frac{\partial\psi_2}{\partial y}=0,\quad \gamma_2=0,\quad \text{at } y=h(x). \tag{53}$$

5.4. Solution for zero order system

$$\psi_0=L_{01}y^5+L_{02}y^3+L_{03}y+L_{04}, \tag{54}$$

$$u_0=5L_{01}y^4+3L_{02}y^2+L_{03}, \tag{55}$$

$$\gamma_0=\frac{1}{2}\left(h^2\beta_1-y^2\beta_1\right), \tag{56}$$

$$\frac{dp_0}{dx}=\left[\frac{-360F-360h+180h^2-12Gth^5\beta_1+60Gth^3y^2\beta_1}{120h^3}+Gt\left(\frac{1}{2}\left(h^2\beta_1-y^2\beta_1\right)\right)\right], \tag{57}$$

$$\Delta P_{\lambda_0}=\int_o^{2\pi}\frac{dp_0}{dx}dx. \tag{58}$$

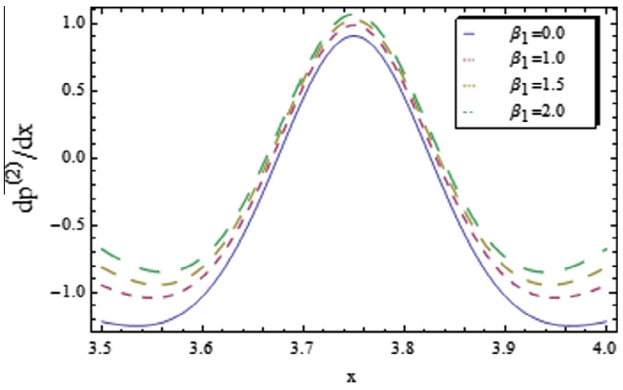

Figure 3 Influence of β_1 on $dp^{(2)}/dx$ when $a = 0.45, \alpha = 0.1$, $Gt = 0.67, \theta = 0.4, \lambda_1 = 0.4,\ \lambda_2 = 0.5$.

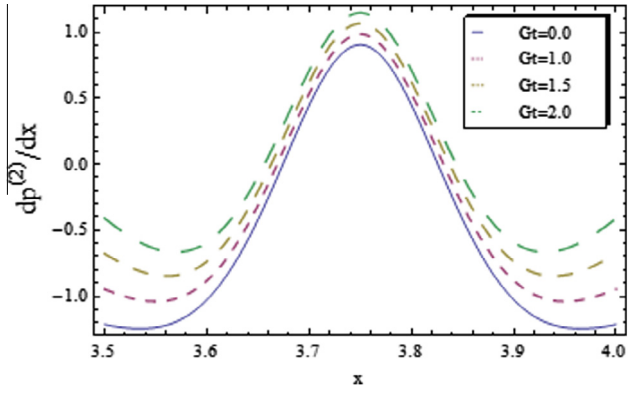

Figure 4 Influence of Gt on $dp^{(2)}/dx$ when $a = 0.45, \beta_1 = 0.67$, $\alpha = 0.1, \theta = 0.4, \lambda_1 = 0.4,\ \lambda_2 = 0.5$.

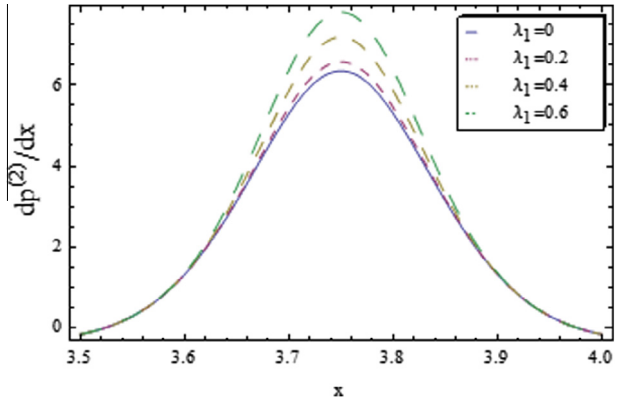

Figure 5 Influence of λ_1 on $dp^{(2)}/dx$ when $a = 0.45, \beta_1 = 0.67$, $Gt = 0.5, \theta = 0.1, \alpha = 0.1,\ \lambda_2 = 0.5$.

5.5. Solution for the first order system

$$\psi_1 = L_{11}y^{11} + L_{12}y^9 + L_{13}y^7 + L_{14}y^5 + L_{15}y^3 + L_{16}y, \tag{59}$$

$$u_1 = 11L_{11}y^{10} + 9L_{12}y^8 + 7L_{13}y^6 + 5L_{14}y^4 + 3L_{15}y^2 + L_{16}, \tag{60}$$

$$\frac{dp_1}{dx} = \frac{1}{144375h^7}\left[\begin{array}{c} -2338875(F+h)^3 + 44550Gth^5(F+h)^2\beta_1 - 1265 \\ Gt^2h^{10}(F+h)\beta_1^2 + 4Gt^3h^{15}\beta_1^3) \end{array}\right], \tag{61}$$

$$\gamma_1 = 0, \tag{62}$$

$$\Delta P_{\lambda_1} = \int_o^{2\pi} \frac{dp_1}{dx}dx. \tag{63}$$

5.6. Solution for the second order system

$$\psi_2 = L_{211}y^{17} + L_{212}y^{15} + L_{213}y^{13} + L_{214}y^{11} + L_{215}y^9 + L_{216}y^7 + L_{217}y^5 + L_{218}y^3 + L_{219}y, \tag{64}$$

$$u_2 = 17L_{211}y^{16} + 15L_{212}y^{14} + 13L_{213}y^{12} + 11L_{214}y^{10} + 9L_{215}y^8 + 7L_{216}y^6 + 5L_{217}y^4 + 3L_{218}y^2 + L_{219}, \tag{65}$$

$$\begin{aligned} \frac{dp_2}{dx} = {} & \frac{1}{175h^{11}}\left(729(12A^2 - 25B)(F+h^5)\right) \\ & - \frac{18}{175h^6}\left(69A^2 - 50B\right)Gt(F+h)^4\beta_1 \\ & + \frac{6}{67375h}\left(Gt^2(F+h)^3\right)\beta_1^2 \\ & - \frac{2\left(13047A^2 - 6650B\right)Gt^3h^4(F+h)^2\beta_1^3}{4379375} \\ & + \frac{\left(38726A^2 - 19075B\right)(F+h)\beta_1^4}{591215625} \\ & - \frac{4\left(14867A^2 - 6650B\right)Gt^5h^{14}\beta_1^4}{251266640625}, \end{aligned} \tag{66}$$

$$\gamma_2 = 0, \tag{67}$$

$$\Delta P_{\lambda_2} = \int_o^{2\pi} \frac{dp_2}{dx}dx, \tag{68}$$

The values of $L_{0i}\ (i = 1, 2, 3, 4), L_{1j}\ (j = 1, 2, \ldots, 6)$, and $L_{2ij}\ (ij = 11, 12, \ldots, 19)$, as appearing in above equations, are not included for reducing the number of pages.

The expressions of $\Delta P_\lambda, dp/dx, \gamma$ and F_λ up to $O(\delta^2)$ are denoted by $\Delta P_\lambda^{(2)}, dp^{(2)}/dx, \gamma^{(2)}, \phi^{(2)}$ and $F_\lambda^{(2)}$. Mathematically

$$\Delta P_\lambda^{(2)} = \Delta P_{\lambda_0} + \alpha\Delta P_{\lambda_1} + \alpha^2\Delta P_{\lambda_2}, \tag{69}$$

$$dp^{(2)}/dx = \frac{dp_0}{dx} + \alpha\frac{dp_1}{dx} + \alpha^2\frac{dp_2}{dx}, \tag{70}$$

$$\psi^{(2)} = \psi_0 + \alpha\psi_1 + \alpha^2\psi_2, \tag{71}$$

$$\gamma^{(2)} = \gamma_0 + \alpha\gamma_1 + \alpha^2\gamma_2, \tag{72}$$

and final expressions for pressure rise per wavelength, pressure gradient, temperature, mass and frictional forces can be obtained from solutions of zero to second order systems.

6. Discussion

Pumping characteristics, heat characteristics, behavior of velocity and trapping have been thoroughly discussed in proceeding subsections. We have carried out the behavior of the solutions for stream function (ψ), velocity (u), temperature ($\gamma^{(2)}$), pressure gradient ($dp^{(2)}/dx$) and pressure rise per wavelength ($\Delta P_\lambda^{(2)}$) for several values of $\alpha, \beta_1, Gt, \lambda_1$ and λ_2.

6.1. Pumping characteristics

The behavior of material parameter α, heat source/sink parameter β_1, Grashof number Gt, relaxation time λ_1 and retardation time λ_2 on $dp^{(2)}/dx$ and $\Delta P_\lambda^{(2)}$ has been investigated. In Fig. 2

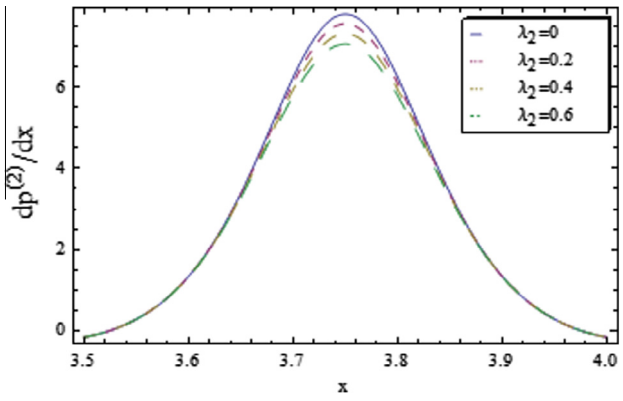

Figure 6 Influence of λ_2 on $dp^{(2)}/dx$ when $a = 0.45, \beta_1 = 0.67, Gt = 0.4, \theta = 0.1, \lambda_1 = 0.5, \alpha = 0.2$.

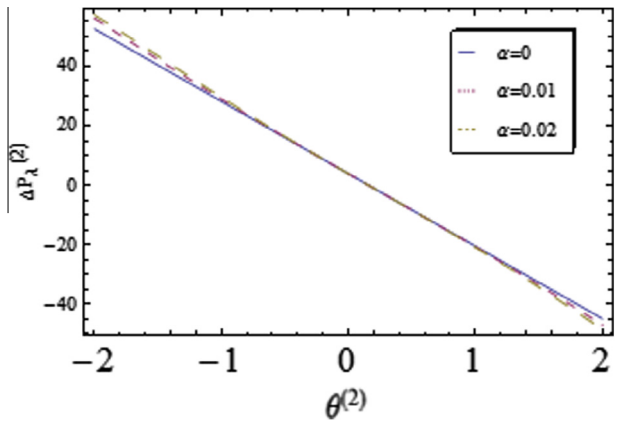

Figure 7 Influence of α on $\Delta P_{\lambda}^{(2)}$ when $Gt = 0.67, a = 0.3, \beta_1 = 0.5, \lambda_1 = 0.4, \lambda_2 = 0.5$.

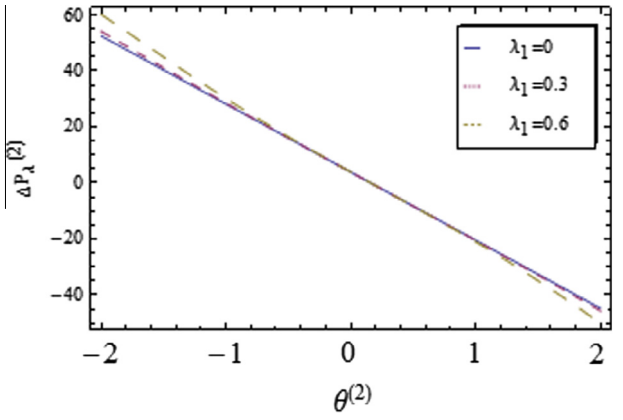

Figure 8 Influence of λ_1 on $\Delta P_{\lambda}^{(2)}$ when $Gt = 0.67, a = 0.3, \beta_1 = 0.5, \alpha = 0.01, \lambda_2 = 0.5$.

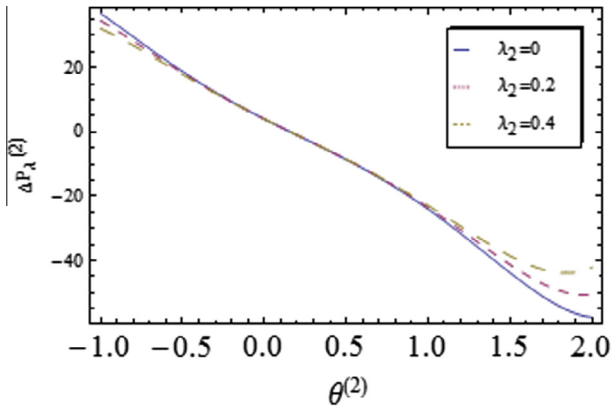

Figure 9 Influence of λ_2 on $\Delta P_{\lambda}^{(2)}$ when $Gt = 1, a = 0.3, \beta_1 = 0.5, \alpha = 0.07, \lambda_1 = 0.5$.

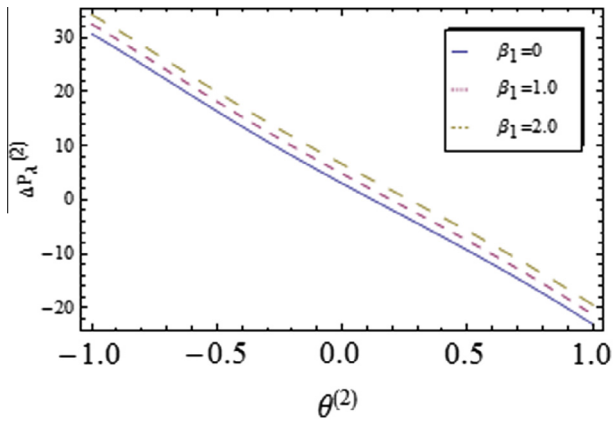

Figure 10 Influence of β_1 on $\Delta P_{\lambda}^{(2)}$ when $Gt = 0.67, a = 0.3, \lambda_1 = 0.5, \alpha = 0.02, \lambda_2 = 0.5$.

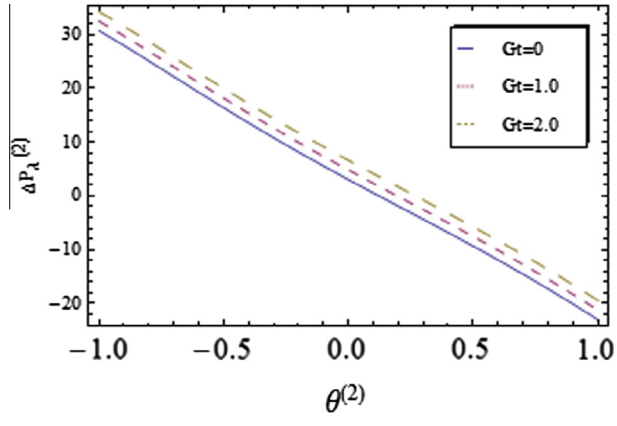

Figure 11 Influence of Gt on $\Delta P_{\lambda}^{(2)}$ when $\alpha = 0.05, a = 0.3, \beta_1 = 0.67, \lambda_1 = 0.4, \lambda_2 = 0.5$.

the variation of $dp^{(2)}/dx$ versus x is shown for different values of α by keeping the other parameters fixed. We can observe that pressure gradient is relatively small in the wider part of the channel. The flow can easily pass through without imposition of large pressure gradient. In spite of a narrow part of the channel there is a need of large pressure gradient to maintain the flux to pass it near $x = 3.75$. In Figs. 3–5 we can get the same behavior as in Fig. 2 for the parameters β_1, Gt and λ_1. In Fig. 6 we can get vice versa behavior for λ_2.

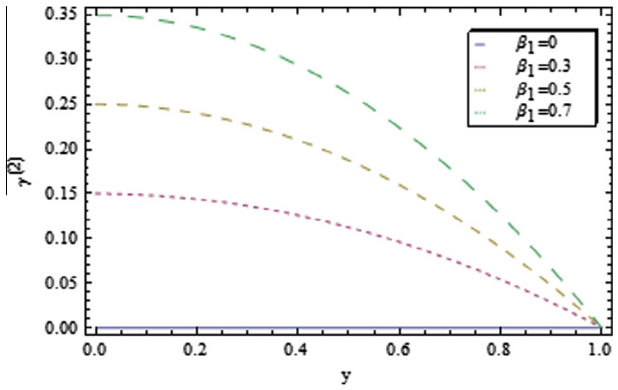

Figure 12 Influence of β_1 on $\gamma^{(2)}$ when $a = 0.5, x = 0.5$.

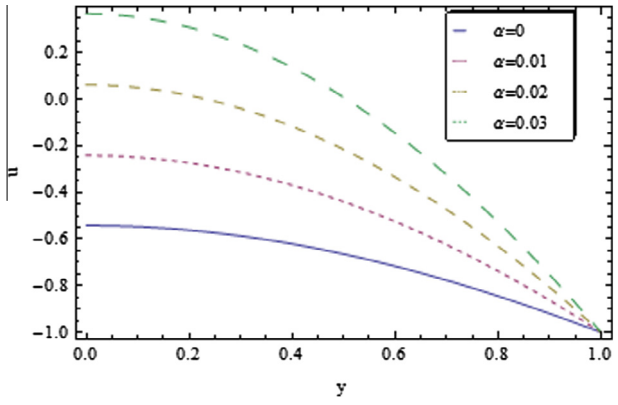

Figure 13 Influence of α on u when $a = 0.3, \lambda_1 = 0.6, \beta_1 = 1$, $Gt = 1$, $x = -1, \lambda_2 = 0.55$.

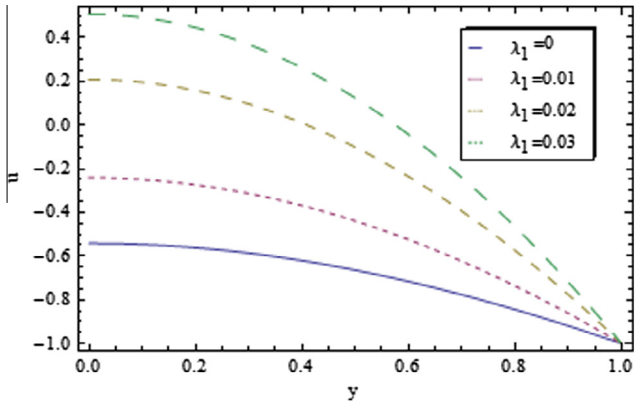

Figure 14 Influence of λ_1 on u when $a = 0.3, \alpha = 0.1, \beta_1 = 1$, $Gt = 1$, $x = -1, \lambda_2 = 1$.

The dimensionless pressure rise per wavelength versus variation of time-averaged flux θ has been plotted in the Figs. 7–11. Here the upper right-hand Quadrant (I) denotes the region of peristaltic pumping, where $\theta^{(2)} > 0$ (positive pumping) and $\Delta P_\lambda^{(2)} > 0$ (adverse pressure gradient). Quadrant (II), where $\Delta P_\lambda^{(2)} < 0$ (favorable pressure gradient)

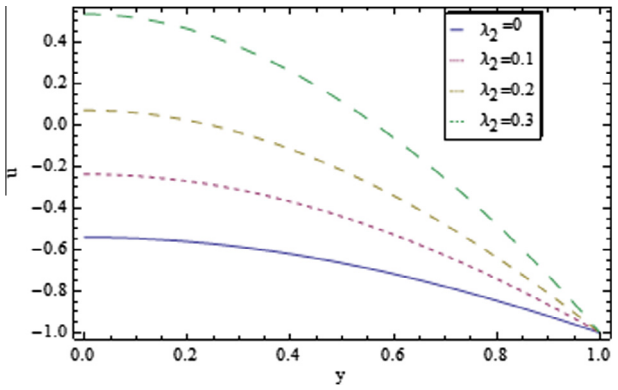

Figure 15 Influence of λ_2 on u when $a = 0.1, \lambda_1 = 1, \beta_1 = 1$, $Gt = 1$, $x = -1, \alpha = 0.2$.

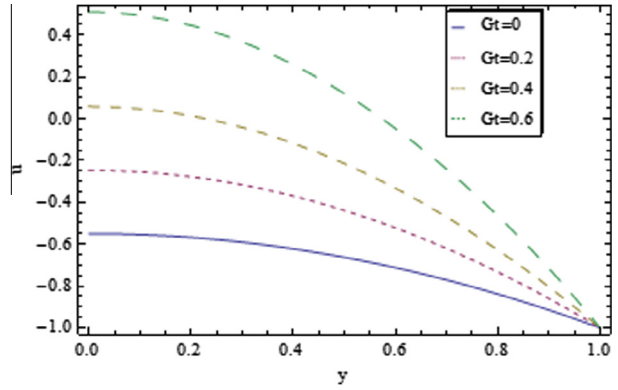

Figure 16 Influence of Gt on u when $a = 0.1, \lambda_1 = 1, \beta_1 = 1$, $\lambda_2 = 1$, $x = -1, \alpha = 0.2$.

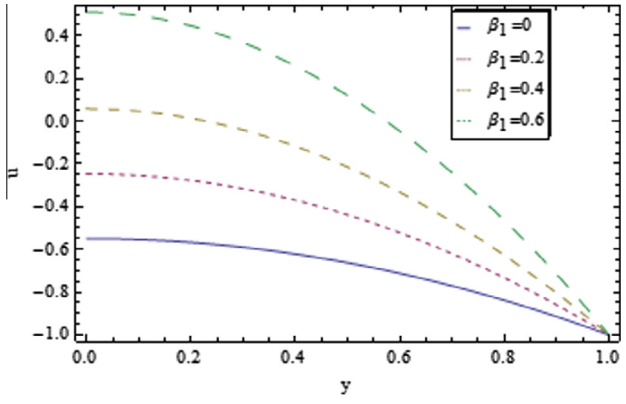

Figure 17 Influence of β_1 on u when $a = 0.2, \lambda_1 = 0.8, \alpha = 0.3$, $Gt = 1$, $x = -1, \lambda_2 = 1$.

and $\theta^{(2)} > 0$ (positive pumping), is designated as augmented flow (copumping region). Quadrant (IV) , such that $\Delta P_\lambda^{(2)} > 0$ (adverse pressure gradient) and $\theta^{(2)} < 0$, is called retrograde or backward pumping. The flow is opposite to the direction of the peristaltic motion, and there is no flow in the last Quadrant (III). Figs. 7 and 8 show that, there is an inverse linear relationship between $\Delta P_\lambda^{(2)}$ and $\theta^{(2)}$, that is, for

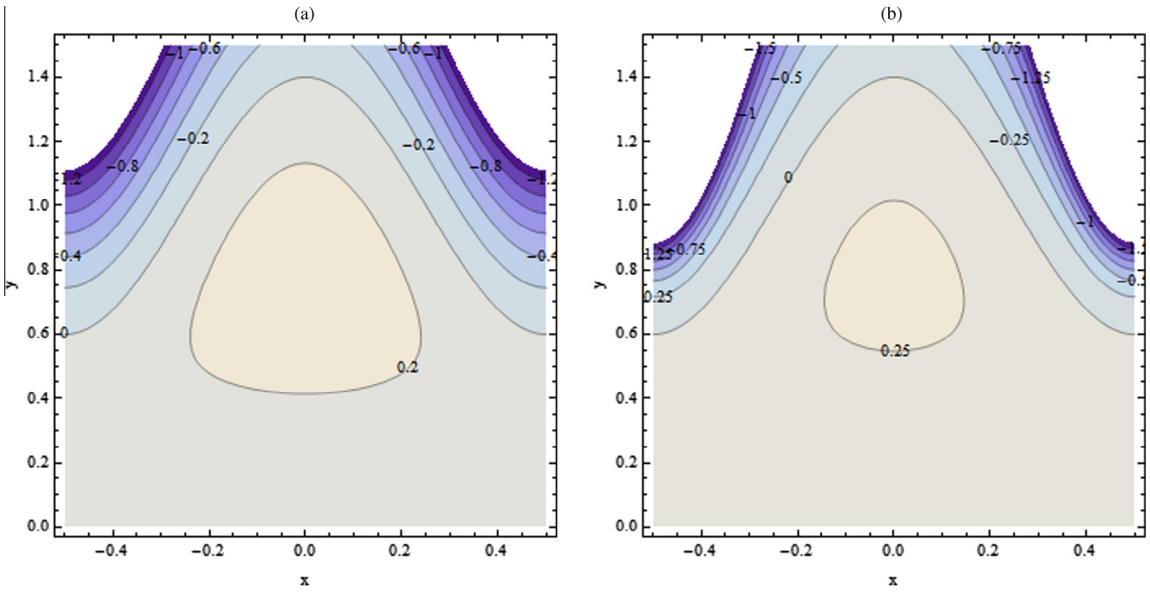

Figure 18 Influence of α on ψ with $a = 0.4, \theta = 1, \lambda_1 = 0.7, \lambda_2 = 0.7, \beta_1 = 1Gt = 0.8(a)\alpha = 0(b)\alpha = 0.1$.

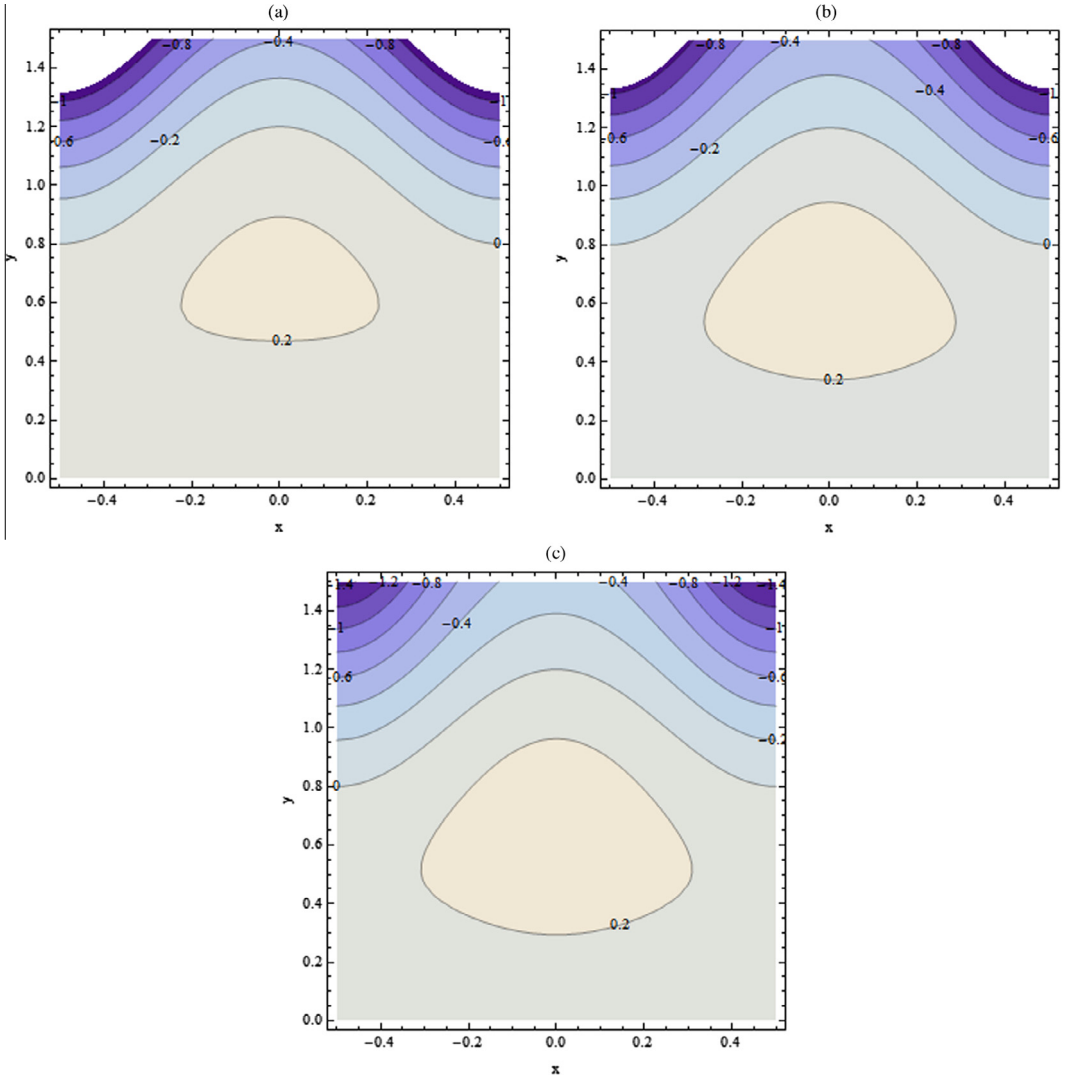

Figure 19 Influence of β_1 on ψ with $a = 0.2, \theta = 1, \lambda_1 = 0.7, \lambda_2 = 0.7, \alpha = 0.01Gt = 1(a)\beta_1 = 0(b)\beta_1 = 0.7(c)\beta_1 = 1.4$.

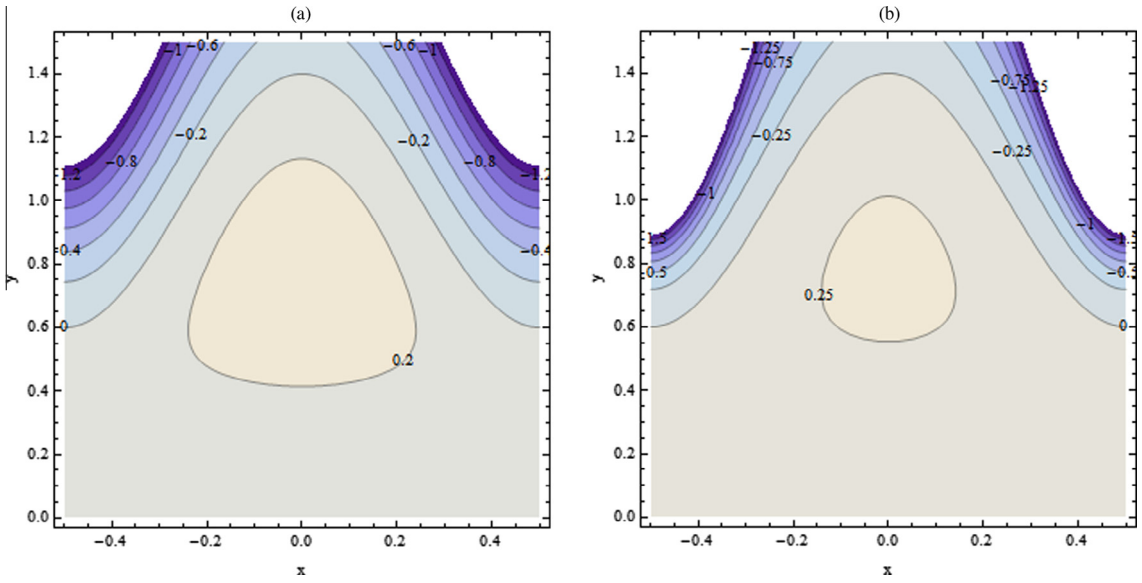

Figure 20 Influence of λ_1 on ψ with $a = 0.4, \theta = 1, \beta_1 = 1, \lambda_2 = 0.7, \alpha = 0.2$ $Gt = 1(a)\lambda_1 = 0(b)\lambda_1 = 0.5$.

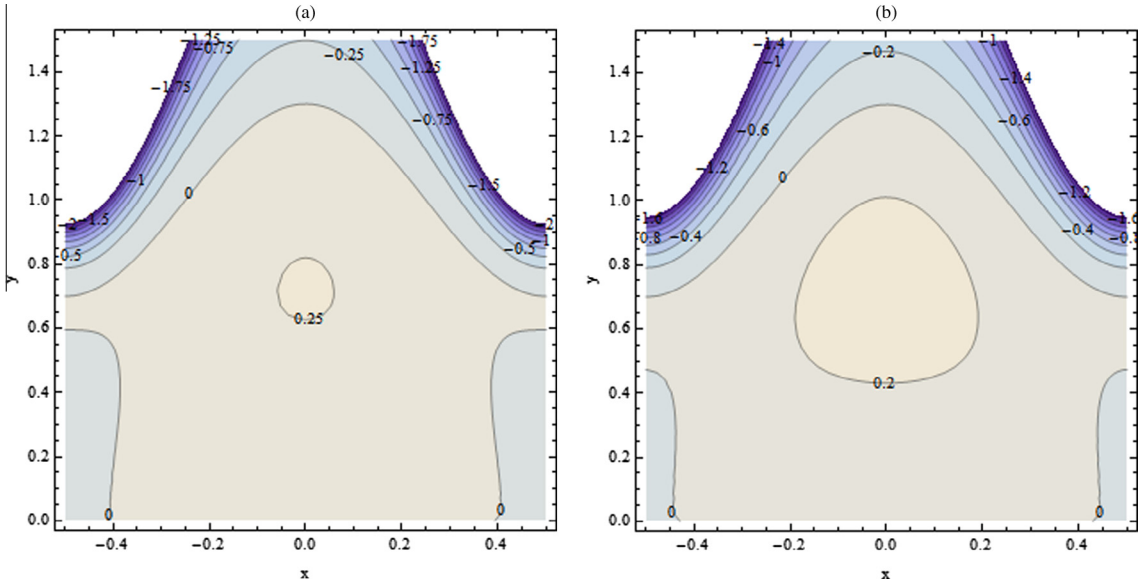

Figure 21 Influence of λ_2 on ψ with $a = 0.3, \theta = 1, \beta_1 = 1, \lambda_1 = 0.7, \alpha = 0.2$ $Gt = 1(a)\lambda_2 = 0(b)\lambda_2 = 0.8$.

the adverse pressure gradient and for the free pumping the pumping increases with the increase in α, and λ_1. On the other hand, in the copumping region, the pumping decreases with the increase of α, and λ_1. In Fig. 9, the pumping decreases with the increase of λ_2 in Quadrant (IV). On the other hand, in Quadrant (II), the pumping increases with the increase of λ_2. In Figs. 10 and 11 we can say that for the adverse pressure gradient, copumping region and for the free pumping, the pumping increases with the increase of β_1 and Gt.

6.2. Heat characteristics

The effect of heat transfer on peristalsis is shown in Fig. 12. In this Fig. it depicts the effect β_1 on the temperature profile $\gamma^{(2)}$ by fixing the other parameters. This figure indicates that the temperature profiles are almost parabolic and temperature increases with the increase of β_1.

6.3. Behavior of velocity

The variations of the material parameter α, heat source/sink parameter β_1, Grashof number Gt, relaxation time λ_1 and retardation time λ_2 on the longitudinal velocity u in the symmetric channel have been plotted in this subsection. All the Figs. show that velocity at the wall has the same value $u(y = h) = -1$ in the wave frame, satisfying the no slip boundary condition for all values of parameters.

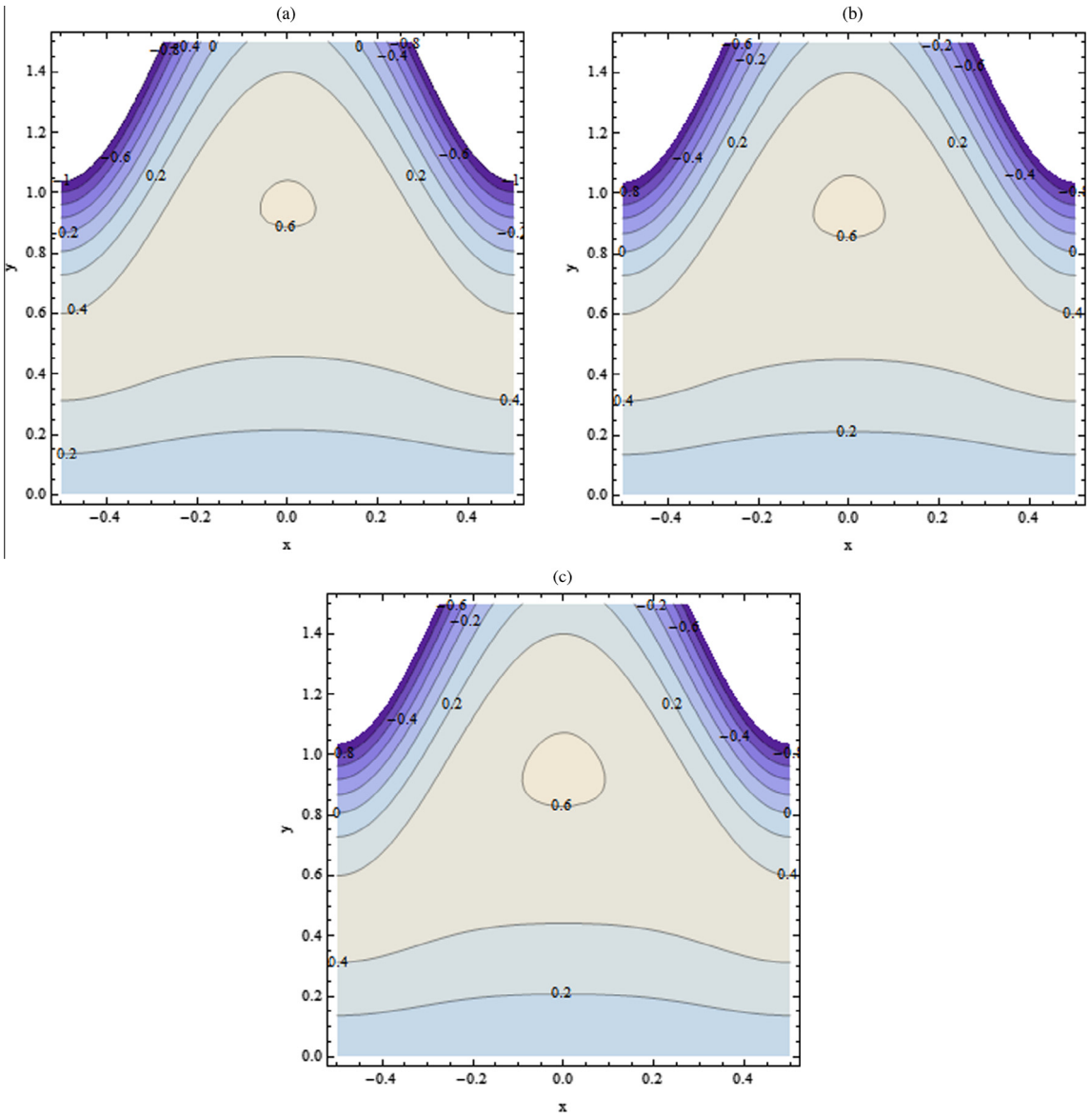

Figure 22 Influence of Gt on ψ with $a = 0.4, \theta = 1.4, \beta_1 = 0.5, \lambda_1 = 0.3, \alpha = 0.01\ \lambda_2 = 0.4 (a) Gt = 1 (b) Gt = 2 (c) Gt = 3$.

Figs. 13–17 give us the result that an increase in $\alpha\ \lambda_1, \lambda_2, Gt$, and β causes an increase in the velocity throughout the channel.

6.4. Trapping

The variation of $\alpha, \beta_1, Gt\ \lambda_1$ and λ_2 is notified in Figs. 18–22. Fig. 18 is plotted for the α. In panel (a) the bolus is symmetric about the center line. Panel (b) shows that the bolus decreases with an increase of α. Fig. 19 is plotted for β_1. Panels (b,c) indicate that the bolus increase with an increase of β_1. Fig. 20 is plotted for λ_1. Panels (b,c) indicate that the bolus decreases with an increase of λ_1. Fig. 21 is plotted for λ_2. Panel (b) shows that the bolus increases with an increase of λ_2. Fig. 22 indicates the same behavior for Gt.

7. Conclusion and future work

The effects of heat transfer on the peristaltic transport of Jeffrey six-constant fluid model have been analyzed. The long wave length and low Reynolds number approximations lead to simplified problem. Analytical solutions have been developed for the stream function, velocity, temperature, pressure gradient, and pressure rise per wavelength. The numerical solutions presented in this paper have been compared with those given in [16]. The results are as follows:

- In the copumping region, the pumping rate decreases by increasing the value of α.
- The longitudinal velocity is an increasing function of α.
- The size of the trapped bolus decreases by increasing the value of α.

- The temperature profile increases by increasing the value of β_1.An interesting idea would be the optimization case in which the location, size and other geometrical parameters of the heat sinks/sources are optimized to reach the best heat sink/source or fluid flow performance. In the literature, Hajmohammade et al. have done a lot of works in this interesting field [17–22]. Hajmohammade et al. have done another great work by considering the power law rule for the fluid flow [23,24].

References

[1] T.W. Latham, Fluid motion in a peristaltic pump (M.Sc. thesis), Massachusetts Institute of Technology, Cambridge, 1966.

[2] K.H.S. Mekheimer, Y. Abd elmabound, Peristaltic flow of a couple stress fluid in an annulus: application of an endoscope, Physica A 387 (2008) 2403–2415.

[3] M. Kotkandapani, S. Srinivas, Nonlinear peristaltic transport of a Newtonian fluid in an inclined asymmetric channel through a porous medium, Phys. Lett. A 372 (2008) 1265–1276.

[4] K. Das, Effects of slip and heat transfer on MHD peristaltic flow in an inclined asymmetric channel, Iran. J. Math. Sci. Inf. 7 (2012) 35–52.

[5] M. kothandapani, S. Srinivas, Peristaltic transport of a Jeffrey fluid under the effect of magnetic field in an asymmetric channel, Int. J. Non-Linear Mech. 43 (2008) 915–924.

[6] G. Radhakrishnamacharya, V.R. Murty, Heat transfer to peristaltic transport in a non-uniform channel, Def. Sci. J. 43 (1993) 275–280.

[7] A. Ogulu, Effect of heat generation on low Reynolds number fluid and mass transfer in a single lymphatic blood vessel with uniform magnetic field, Int. Commun. Int. J. Heat Mass Transfer 33 (2006) 90–799.

[8] S. Srinivas, M. Kothandapani, The influence of heat and mass transfer on MHD peristaltic flow through a porous space with compliant walls, Appl. Math. Comput. 213 (2009) 197–208.

[9] D. Tripathi, S.K. Pandey, O.A. Beg, Mathematical modelling of heat transfer effects on swallowing dynamics of viscoelastic food bolus through the human oesophagus, Int. J. Therm. Sci. 70 (2013) 41–53.

[10] Kh.S. Mekheimer, Y.A. Elmabound, The influence of heat transfer and magnetic field on peristaltic transport of a Newtonian fluid in a vertical annulus: application of an endoscope, Phys. Lett. A 372 (2008) 1657–1665.

[11] C. Vasudev, U. Rajeswara Rao, M.V. Subba Reddy, G. Prabhakara Rao, Effects of heat transfer on the peristaltic flow of Jeffrey fluid through a porous medium in a vertical annulus, J. Basic. Appl. Sci. Res. 1 (2011) 751–758.

[12] A.A. Khan, R. Ellahi, K. Vafai, Peristaltic transport of a Jeffrey fluid with variable viscosity through a porous medium in an asymmetric channel, http://dx.doi.org/10.1155/2012/169642.

[13] S. Akram, S. Nadeem, Significance of nanofluid and partial slip on the peristaltic transport of a Non-Newtonian fluid with different waveforms 13 (2014) 375–385.

[14] S.K. Pandey, D. Tripathi, Unsteady model of transportation of Jeffrey fluid by peristalsis, Int. J. Biomath. 3 (2010) 473–491.

[15] N.S. Akbar, S. Nadeem, Z.H. Khan, Thermal and velocity slip effects on the MHD peristaltic flow with carbon nanotubes in an asymmetric channel: application of radiation therapy, <http://link.springer.com/artical/10.1007%2Fs13204-013-0265-2/fulltext.html>.

[16] S. Noreen, Numerical study of an induced magnetic field on the peristaltic flow of a Jeffrey six-constant fluid, Eur. Phys. J. Plus 129 (2014) 35.

[17] M.R. Hajmohammadi, A. Campo, S.S. Nourazar, A.M. Ostad, Improvement of forced convection cooling due to the attachment of heat sources to a conducting thick plate, J. Heat Transfer ASME 135 (2013) 124504–124511.

[18] M.R. Hajmohammadi, O.J. Shariaatzadeh, M. Moulod, S.S. Nourazar, Phi and Psi shaped conductive routes for improved cooling in a heat generating piece, Int. J. Therm. Sci. 77 (2014) 66–77.

[19] M.R. Hajmohammadi, v.A. Abianeh, M. Moezzinahafabadi, M. Daneshi, Fork-shaped highly conductive pathways for maximum cooling in a heat generating piece, Appl. Therm. Eng. 61 (2013) 228–235.

[20] M.R. Hajmohammadi, E. Shirani, M.R. Salimpour, A. Campo, Constructal placement of unequal heat sources on a plate cooled by laminar forced convection, Int. J. Therm. Sci. 60 (2012) 13–22.

[21] M.R. Hajmohammadi, S. Poozesh, S.S. Nourazar, A.H. Manesh, Optimal architecture of heat generating pieces in a fin, J. Mech. Sci. Technol. 27 (2013) 1143–1149.

[22] M.R. Hajmohammadi, S. Poozesh, S.S. Nourazar, Constructal design of multiple heat sources in a square-shaped fin, J. Process. Mech. Eng. 226 (2012) 324–336.

[23] M.R. Hajmohammadi, S.S. Nourazar, On the insertion of a thin gas layer in micro cylinder Coutte flows involving power-law fluids, Int. J. Heat Mass Transfer 75 (2014) 97–108.

[24] M.R. Hajmohammadi, S.S. Nourazar, A. Campo, Analytical solution for two-phase flow between two rotating cylinders filled with power law liquid and a micro layer of gas, J. Mech. Sci. Technol. 28 (2014) 1849–1854.

[25] N.S. Akbar, S. Nadeem, Z.H. Khan, Numerical simulation of peristaltic flow of a Carreau nanofluid in an asymmetric channel, Alex. Eng. J. 53 (2014) 191–197.

[26] A. Riaz, R. Ellahi, S. Nadeem, Peristaltic transport of a Carreau fluid in a compliant rectangular duct, Alex. Eng. J. 53 (2014) 475–484.

[27] M. Qasim, Heat and mass transfer in a Jeffrey fluid over a stretching sheet with heat source/sink, Alex. Eng. J. 52 (2013) 571–575.